EPJ Web of Conferences **202**, 02002 (2019) https://doi.org/10.1051/epjconf/201920202002
CHARM 2018

Experimental Status of Conventional Charmonium Spectroscopy

Xiongfei Wang[1,*]

[1]Institute of High Energy Physics, Beijing 100049, People's Republic of China

Abstract. Based on data samples taken by the BESIII, Belle, KEDR and LHCb experiments, many measurements on conventional charmonium spectroscopy were finished in the past years. Some of recent results, such as precise measurements of J/ψ and $\psi(2S)$ masses, the J/ψ decay width, the J/ψ and $\psi(2S)$ electronic widths, two-photon width of $\chi_{c0,2}$ meson, the $\chi_{c1,2}$ resonance parameters with the decays $\chi_{c0,2} \to J/\psi\mu^+\mu^-$, the η_c resonance parameters and observations of $X(3823)$ and $X^*(3860)$, were reported.

1 Introduction

Shortly after the discovery of J/ψ, Appelquist and Politer [1] proposed that if there existed a heavy charm quark, it should form a nonrelativistic bound state of charmed quark and anti-charm quark ($c\bar{c}$) with a similar spectrum of energy levels to the positronium, which then was called charmonium taking into account beautifying the language. The first member, J/ψ meson with hidden charm, which was quickly identified as the 1^3S_1 state of charmonium. Subsequently, many new charmonium states $\eta_c(1S)$, χ_{cJ}, $\psi(2S)$, $\psi(3773)$, $\psi(4040)$, $\psi(4260)$, $\psi(4360)$, $\psi(4415)$, $\psi(4660)$, etc., produced from e^+e^- annihilation via a virtual photon one after another were found [2], in which $\psi(4260)$, $\psi(4360)$ $\psi(4660)$, were originally thought to be charmonium states, but some of current evidences and theoretical predictions suggested more exotic explanations, such as a tetraquark state, a molecule or a hybird meson [3]. Other states, such as $\eta_c(1S)$, χ_{cJ}, J/ψ, $\psi(2S)$, $\psi(3773)$, $\psi(4040)$, $\psi(4160)$, $\psi(4415)$, etc., were thought to be pure charmonium states, it is sometimes called conventional charmonium state (CCS) because for these CCS, the observations of their spectroscopies are basically consistent with the predictions from potential models and lattice quantum chromodynamics (QCD) [4].

2 Experimental apparatus

2.1 The BESIII experiment

The BESIII experiment is dedicated to the τ-charm physics at the Beijing Electron Position Collider (BEPCII) [5]. The detector is a magnetic spectrometer and its cylindrical core consists of a helium-based multilayer drift chamber (MDC), a plastic scintillator time-of-flight system (TOF), and a CsI(Tl) electromagnetic calorimeter (EMC), which are all enclosed in a superconducting solenoidal magnet (SSM) providing a 1.0 T (0.9 T in 2012) magnetic field.

*e-mail: wangxf@ihep.ac.cn

The solenoid is supported by an octagonal flux-return yoke with resistive plate counter muon identifier modules interleaved with steel. The acceptance of charged particles and photons is 93% over 4π solid angle. The charged-particle momentum resolution at 1 GeV/c is 0.5%, and the dE/dx resolution is 6% for the electrons from Bhabha scattering. The EMC measures photon energies with a resolution of 2.5% (5%) at 1 GeV in the barrel (end cap) region. The time resolution of the TOF barrel part is 68 ps, while that of the end cap part is 110 ps. The end cap TOF system is upgraded in 2015 with multi-gap resistive plate chamber technology, providing a time resolution of 60 ps [6]. Figure 1 shows a schematic view of the BESIII detector. A detailed description of the BESIII detector is given in Ref. [7].

Up to now, the BESIII detector due to the excellent performance has collected the world largest data samples, i.e. 1.3×10^9 J/ψ events [8], 448×10^{-6} $\psi(2S)$ events [9], 2.9 fb^{-1} $\psi(3773)$ events [10], 1.0 fb^{-1} R scan events with 131 center-of-mass (CM) energy points [11] and 5.0 fb^{-1} XYZ data events [12].

2.2 The Belle experiment

The Belle experiment is dedicated to search for CP violation and extends to the studies of rare decays of B meson at $\Upsilon(4S)$ resonance [13]. The detector is a large solid-angle magnetic spectrometer that consists of a silicon vertex detector (VTX), a 50-layer central drift chamber, an array of aerogel threshold Cherenkov counters, a barrel- like arrangement of TOF scintillation counters, and an EMC comprised of CsI(Tl) crystals located inside a SSM that provides a 1.5 T magnetic field. An iron flux-return yoke instrumented with resistive plate chambers (KLM) located outside the coil is used to detect KL0 mesons and to identify muons. The Belle detector is described in detail elsewhere [14]. Figure 1 shows an overview of the Belle detector. The integrated luminosities [15] collected by the Belle detector are 100 fb^{-1} scan data, 6 fb^{-1} at $\Upsilon(1S)$, 25 fb^{-1} at $\Upsilon(2S)$, 3 fb^{-1} at $\Upsilon(3S)$, 711 fb^{-1} at $\Upsilon(4S)$ and 121 fb^{-1} at $\Upsilon(4S)$.

2.3 The KEDR experiment

The KEDR experiment is dedicated to study the c, b-quarks physics region employed at the VEPP-4M e^+e^- collider [16, 17]. The detector includes a tracking system consisting of a VTX and a MDC, a PID system of aerogel Cherenkov counters and TOF scintillation counters, and an EMC based on liquid krypton (barrel part) and CsI crystals (end cap part). The SSM provides a longitudinal magnetic field of 0.6 T. A muon system is installed inside the magnet yoke. The detector also includes a high-resolution tagging system for studies of two-photon processes. Figure 1 shows an overview of the KEDR detector.

2.4 The LHCb experiment

The LHCb experiment is dedicated to heavy flavor physics at the Large Hadron Collider (LHC) at CERN [18], its primary purpose is to look for indirect evidence of new physics in CP violation and rare decays of B hadrons. The detector is a single-arm forward spectrometer covering the pseudorapidity range $2 < \eta < 5$. It includes a high-precision tracking system consisting of a silicon- strip VTX surrounding the pp interaction region, a large-area silicon-strip detector located upstream of a dipole magnet with a bending power of about 4 Tm, and three stations of silicon-strip detectors and straw drift tubes placed downstream of the magnet. The LHCb detector is described in detail [19]. Figure 1 shows an overview of the LHCb detector. The integrated luminosities [20] recorded by the LHCb detector are 1.1 fb^{-1} at 7 TeV in 2011, 2.1 fb^{-1} at 8 TeV in 2012, and about 4 fb^{-1} at 13 TeV from 2015 up to now, and the plan is to accumulate up to 5 fb^{-1} at 13 TeV by the end of 2018.

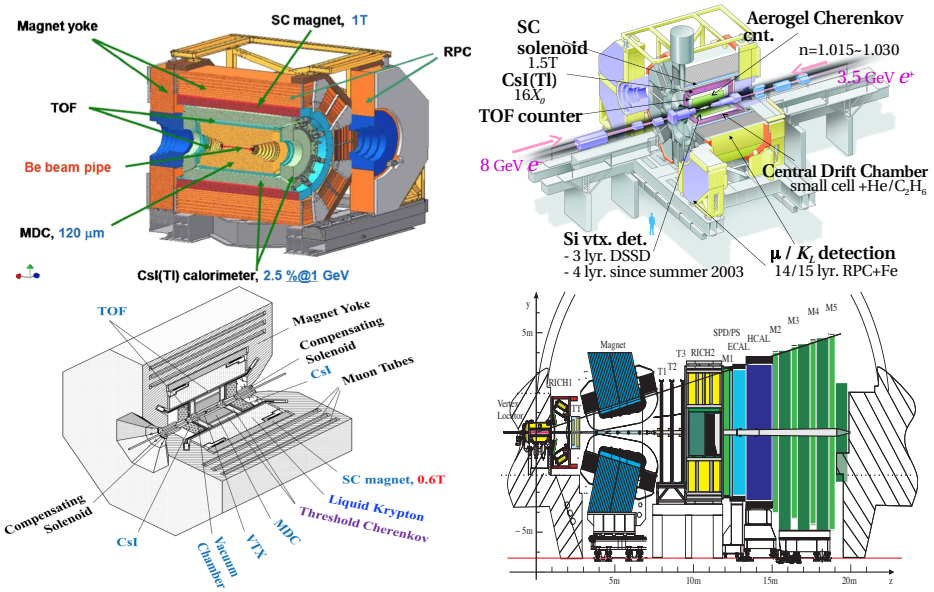

Figure 1. Schematic drawing of the detectors for BESIII (Top left) [7], Belle (Top right) [14], KEDR (Bottom left)[17] and LHCb (Bottom right) [19] showing its main components.

3 Recent CCS results

3.1 The J/ψ and $\psi(2S)$ resonance parameters

3.1.1 Precise measurements of J/ψ and $\psi(2S)$ masses

The mass of a particle is its most fundamental characteristic, which should be known with the best possible accuracy. The masses of J/ψ and $\psi(2S)$ are usually used to calibrate the energy scales of accelerators and detectors operation in the charmonium region. The measurement precision of J/ψ and $\psi(2S)$ masses is helpful to determine the accuracy of masses of other charmonium states and the τ-lepton. In history, the J/ψ and $\psi(2S)$ masses were measured by many experiments [2], and achieved an accuracy of 17 MeV reported by KEDR experiment with the installment of the liquid krypton combined with data samples of additional three $\psi(2S)$ scans [21]. Recently, the KEDR experiment presented the best precise measurements for the J/ψ and $\psi(2S)$ masses, i.e. $M_{J/\psi}$ = (3096.900 ± 0.002 ± 0.006) MeV/c^2, $M_{\psi(2S)}$ = (3686.099±0.004±0.009) MeV/c^2, based on data samples of six J/ψ scans and seven $\psi(2S)$ scans [22] using the resonance depolarization method. Figure 2 shows the fitted hadronic cross section for J/ψ scans and $\psi(2S)$ scans from different years.

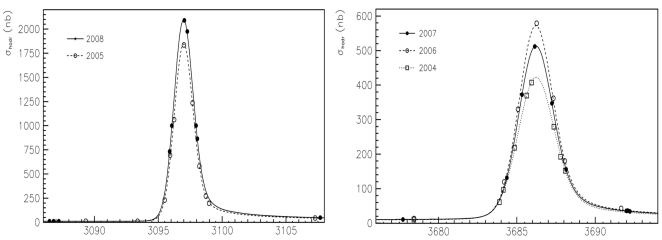

Figure 2. The measured hadronic cross section without the correction of the detection efficiency as a function of the CM energy for J/ψ scans (Left) and $\psi(2S)$ scans (Right) [22]. The lines present the fit results.

3.1.2 Precise measurements of J/ψ and $\psi(2S)$ electronic widths

The electronic width of the J/ψ resonance is also an interesting and important parameter, which could reveal the basic structure of J/ψ resonance. It was measured first by BaBar [23] and CLEO-c [24] with the technique of initial state radiation (ISR). In 2015, the BESIII experiment performed additionally a search for the reaction $e^+e^- \to \gamma_{ISR}X(3872) \to \gamma_{ISR}\pi^+\pi^- J/\psi$ via ISR technique [25]. No obvious significance of $X(3823)$ was observed in this process, and an improved limit $\Gamma_{ee}^{X(3823)}\mathcal{B}(X(3823) \to \pi^+\pi^- J/\psi) < 0.13$ eV was given. Theoretically, the production of a resonance with quantum numbers $J^{PC} = 1^{++}$, such as the $X(3872)$, via single photon e^+e^- annihilation is forbidden, but is allowed by a next-to-leading order box diagram. Additionally, in this analysis, the $\psi(2S)$ electronic width was measured by fitting $M(\pi^+\pi^- J/\psi)$ spectrum, i.e. $\Gamma_{ee}^{\psi(2S)} = (2213 \pm 18 \pm 99)$ eV, which is in agreement with the world average value [2] and updated the previous measurement [27]. Subsequently, the BESIII experiment measured the J/ψ electronic width with more precise accuracy using the ISR process $e^+e^- \to J/\psi\gamma \to \mu^+\mu^-\gamma$ by fitting $m(\mu^+\mu^-)$ spectrum in the range of 2.8 and 3.4 GeV/c^2, i.e. $\Gamma_{ee}^{J/\psi} = (5.58 \pm 0.05 \pm 0.08)$ keV [26]. Figure 3 shows the fitted mass spectra of $\mu^+\mu^-$ and $\pi^+\pi^- J/\psi$.

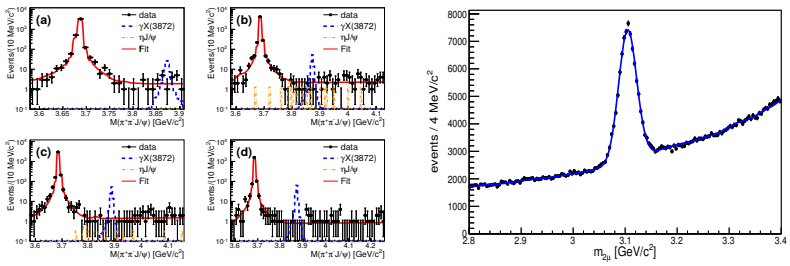

Figure 3. (Left) Fit to the distribution of $M(\pi^+\pi^- J/\psi)$ [25]. (Right) Fit to the distribution of $m_{\mu^+\mu^-}$ [26]. The solid line is the fit result. The dots with error bar are the data. The lines present the fit results.

3.1.3 Precise measurement of J/ψ width

The J/ψ width is an important parameter and reflect the internal interaction of J/ψ meson, which was predicted by various potential models and QCD. Thus, precise measurements of J/ψ decay widths may help validate these models and provide a better understanding of the underlying physics. In history, the J/ψ width was measured by many experiments [2] achieved an accuracy of 2.8 keV [2]. Recently, the BESIII experiment performed a more accurate measurement of J/ψ (lepton) width with processes $e^+e^- \to e^+e^-$, $\mu^+\mu^-$ at 15 CM energy points in the vicinity of the J/ψ resonance, i.e. $\Gamma_{tot} = (94.3 \pm 2.1)$ keV and $\Gamma_{ll} = (5.64 \pm 0.11)$ keV. These results are consistent with and of improved precision with respect to those from other experiments, but a bit less precise than the previous BESIII result obtained with the ISR technique. Figure 4 shows the comparison of full width and lepton width of J/ψ between this work and other measurements.

3.2 The $\chi_{cJ}(1P)$ resonance parameter

3.2.1 Precise measurement of $\chi_{c0,2}$ two-photon width

The two-photon decays of P-wave charmonia, such as the decays $\chi_{c0,2} \to \gamma\gamma$, are helpful for understanding the nature of inter-quark forces and decay mechanisms, where the decay $\chi_{c1} \to$

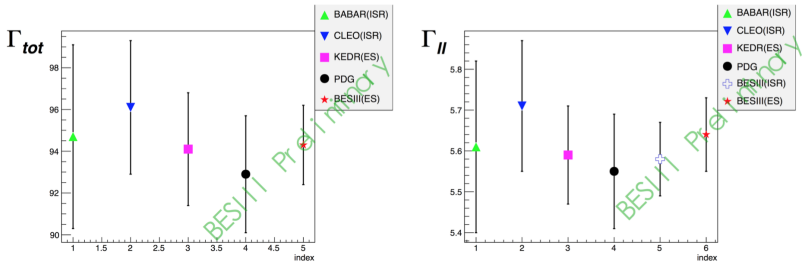

Figure 4. Comparisons of full width and lepton width of J/ψ meson for the preliminary BESIII results and other previous measurements [2].

$\gamma\gamma$ is suppressed by Landau-Yang theorem [28]. In particular, the decays $\chi_{c0,2} \to \gamma\gamma$ offer the closest parallel between quantum electrodynamics (QED) and QCD, being analogous to the decays of the triplet states of positronium. One of interesting variables for $\chi_{c0,2} \to \gamma\gamma$ is the ratio of the two-photon decay widths $\frac{\Gamma(\chi_{c2}\to\gamma\gamma)}{\Gamma(\chi_{c0}\to\gamma\gamma)}$, which is predicted by many theoretical models covering a wide range of values between 0.09 and 0.36 [29]. The two-photon decay widths of $\chi_{c0,2}$ were measured by many experiments [2]. Recently, the BESIII experiment performed an improved measurement of two-photon width of $\chi_{c0,2}$ and a helicity amplitude analysis of $\chi_{c2} \to \gamma\gamma$ based on 448 million $\psi(2S)$ events with the process $\psi(2S) \to \gamma\chi_{cJ}$, $\chi_{cJ} \to \gamma\gamma$ [30]. Figure 5 shows the fitted $E(\gamma_1)$ spectrum. The measured ratio of two-photon width of $\chi_{c0,2}$ confirmed that helicity-zero component is highly suppressed. These results are more precise to data, and consistent with previous measurements [2].

3.2.2 Measurement of $\chi_{c1,2}$ resonance parameter

As mentioned in Sec. 3.1, the mass and width of a resonance are the most fundamental characteristics. Recently, the LHCb experiment presented an observation of $\chi_{c1,2} \to J/\psi\mu^+\mu^-$ using $J/\psi \to \mu^+\mu^-$ decay [31]. The parameters of $\chi_{c1,2}$ meson were measured to be $m(\chi_{c1}) = (3510.71 \pm 0.04 \pm 0.09)$ MeV/c^2, $m(\chi_{c2}) = (3556.10 \pm 0.06 \pm 0.11)$ MeV/c^2 and $\Gamma(\chi_{c2}) = (2.10 \pm 0.20 \pm 0.02)$ MeV, respectively. These results are in good agreement with and have comparable precision to the current world averages [2]. Figure 5 shows the fitted distribution of $m(J/\psi\pi^+\pi^-)$. The observations presented here open up a new avenue for hadron spectroscopy at the LHC experiment, such as measurement of $\chi_{c1,2}$ production and even measurement down to very low p_t probing further QCD predictions.

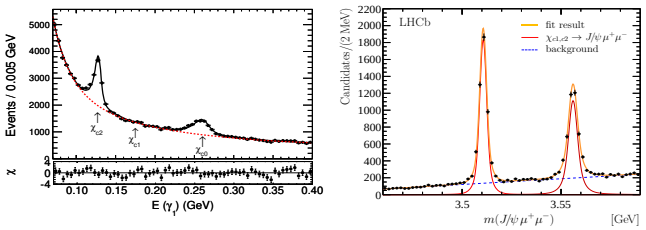

Figure 5. (Left) Fit to the energy spectrum of radiation photon [30]. (Right) Fit to the invariant mass of $J/\psi\pi^+\pi^-$ [31]. Dots with error bar are for the data. The solid line denotes the fit results. The dashed line stands for the backgrounds.

3.3 The $\eta_c(1S)$ resonance parameter

The $\eta_c(1S)$ state is the lowest-lying S-wave spin-singlet charmonium state and has been observed in various processes [2]. Recently, the KEDR experiment performed the measure-

ments of decay rate $\Gamma^0_{\gamma\eta_c(1S)} = (2.98 \pm 0.18^{+0.15}_{-0.33})$ keV and resonance parameters $M(\eta_c(1S)) = (2983.5 \pm 1.4^{+1.6}_{-3.6})$ MeV/c^2, $\Gamma_{\eta_c(1S)} = (27.2 \pm 3.1^{+5.4}_{-2.6})$ MeV, using the inclusive photon spectrum of a magnetic dipole radiative transition decay $J/\psi \to \gamma\eta_c(1S)$ with consideration of an asymmetric photon line-shape [17]. The measured decay rate is significantly higher compared to those previous measurements [2], but is well consistent with the latest lattice QCD prediction [32]. It is noted that the measured parameters are sensitive to the line-shape of the photon spectrum in this decay and it was taken into account during analysis. Subsequently, the LHCb experiment also reported a measurement of $\eta_c(1S)$ width by fitting $M_{p\bar{p}}$ spectrum using the process $B^+ \to p\bar{p}K^+$ based on pp collision data, $\Gamma_{\eta_c(1S)} = (34 \pm 1.9 \pm 1.3)$ MeV [33]. Additionally, the $\eta_c(2S) \to p\bar{p}$ was observed first with a total significance of 6.0σ, and the upper limits of relative branching fraction for other processes $\psi(3773)$, $X(3823) \to p\bar{p}$ were determined. Compared with the results obtained by radiative decays [17], the determinations of $\eta_c(1S)$ parameters do not depend on the knowledge of the line shapes of the magnetic dipole transition. Figure 6 shows the fitted distributions of photon energy and $M_{p\bar{p}}$.

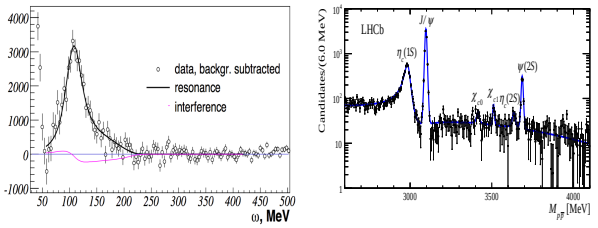

Figure 6. (Left) Fit to the energy spectrum of radiation photon for the process $J/\psi \to \gamma\eta_c$ [17]. (Right) Fit to the invariant mass of $p\bar{p}$ in the process $B^+ \to p\bar{p}K^+$ [33]. Dots with error bar are for the data. The solid line denotes the fit results.

3.4 Observations of $X(3823)$ and $X^*(3860)$

In the charmonium family, the observation of D-wave $c\bar{c}$ meson and its decay modes would test phenomenological models predicted that the as-yet undiscovered 1^3D_2 (ψ_2) has large decay width to $\gamma\chi_{c1}$ and $\gamma\chi_{c2}$ [34]. In 1994, the E705 experiment reported an indication of a 1^3D_2 state with a mass of (3826 ± 13) MeV/c^2 and a statistical significance of 2.8 σ [35]. Recently, the Belle experiment reported a evidence of a new resonance in the $\gamma\chi_{c1}$ final state using the process $B^\mp \to (\gamma\chi_{c1,2})K^\mp$ with a mass of $(3823.1 \pm 1.8 \pm 1.7)$ MeV/c^2 and a significance of 3.8 σ. The measured properties of the $X(3823)$ are consistent with those expected for the $\psi_2(1^3D_2)$ state [36]. Subsequently, the BESIII experiment reported the observation of $X(3823)$ with a mass of $(3821.7 \pm 1.3 \pm 0.7)$ MeV/c^2 and a significance of 6.2 σ using the process $e^+e^- \to \pi^+\pi^- X(3823) \to \pi^+\pi^-\gamma\chi_{c1}$ based on data samples taken at CM energies of 4.230, 4.260, 4.360, 4.420 and 4.600 GeV [37]. These measurements are in good agreement with Belle's measurement and the assignment of the $X(3823)$ state as the $\psi_2(1^3D_2)$ charmonium state. Figure 7 shows the fitted distributions of $M_{\chi_{c1}\gamma}$ and $M_{\rm recoil}(\pi^+\pi^-)$ from Belle and BESIII experiments.

Another new charmoniumlike state $X^*(3860)$ was observed by Belle experiment based on a full amplitude analysis using the process $e^+e^- \to J/\psi D\bar{D}$ ($D \in D^0$ or D^+) with a mass of (3860^{+26+40}_{-32-13}) MeV/c^2 and a width of $(201^{+154+88}_{-67\ -82})$ MeV [38]. The $J^{PC} = 0^{++}$ hypothesis is favored over the 2^{++} hypothesis at the level of 2.5σ. The $X^*(3860)$ seems to be a better candidate for the $\chi_{c0}(2P)$ charmonium state than the $X(3915)$ according to the prediction of the potential model, since its properties are well matched to the expectations for the $\chi_{c0}(2P)$ resonance, where the $X(3915)$ was identified as the $\chi_{c0}(2P)$ candidate in the previous PDG table [39]. Note that, the production amplitudes for the $X^*(3860)$ and $\chi_{c0}(2P)$ are in mutual agreement, but they do not agree with the NRQCD prediction [40]. Figure 8 shows the projection of the fit results onto $M_{D\bar{D}}$.

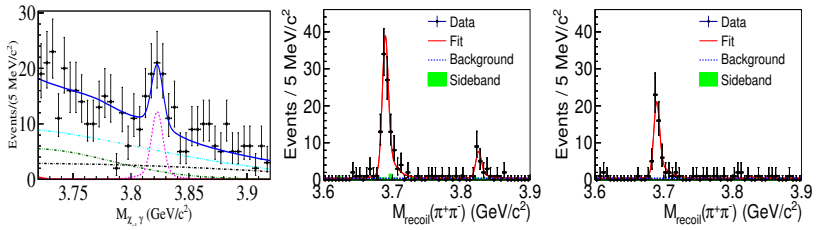

Figure 7. (Left) 2D UML fit projection of the $M_{\chi_{c1}\gamma}$ distribution for the simultaneous fit of $B^{\pm} \to (\chi_{c1}\gamma)K^{\mp}$ and $B^0 \to (\chi_{c1}\gamma)K^0_S$ decays for $M_{\rm bc} > 5.27$ GeV/c^2 [35]. Simultaneous fit to the $M_{\rm recoil}(\pi^+\pi^-)$ distribution of $\gamma\chi_{c1}$ events (Middle) and $\gamma\chi_{c1}$ events (Right) [37]. Dots with error bar are for the data. The solid line denotes the fit results.

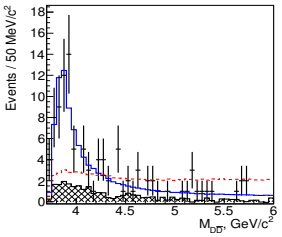

Figure 8. Projection of the signal fit result in the default model onto $M_{D\bar{D}}$ [38]. The hatched histograms are the background, the blue solid line is the fit with a new $X^*(3860)$ resonance ($J^{PC} = 0^{++}$), and the red dashed line is the fit with non-resonant amplitude only. It is noted that the fitted results are consistent with the pure S-wave production of the $X^*(3860)$.

4 Summary

Using data samples taken by BESIII, Belle, KEDR and LHCb experiment, lots of recent progresses in the experimental study of CCS were reported, They include precise measurements of resonance parameters of J/ψ and $\psi(2S)$ mesons, two-photon width of $\chi_{c0,2}$ meson, resonance parameter of $\chi_{c1,2}$ meson, resonance parameter of η_c meson and observations of $X(3823)$ and $X^*(3860)$. In addition, the BESIII, Belle, KEDR and LHCb experiments will continue the study of CCS, and the Belle II at KEK are taking data now. It is hopeful that more progresses will be made in the experimental study of CCS in the future.

5 Acknowledgements

This work is supported in part by Postdoctoral Natural Science Foundation of China under Contract No. 2018M630206; National Natural Science Foundation of China under Contract No. 11521505; Chinese Academy of Science Focused Science Grant; National 1000 Talents Program of China.

References

[1] T. Appelquist *et al.*, Phys. Rev. Lett. **34** 43 (1975); Phys. Rev. D **12** 1404 (1975).

[2] M. Tanabashi *et al.* (Particle Data Group), Phys. Rev. D **98**, 030001 (2018).

[3] C. Z. Yuan, Int. J. Mod. Phys. A **33**, 1830018 (2018); F. K. Guo *et al.*, Rev. Mod. Phys. **90**, 015004 (2018).

[4] S. Godfrey and N. Isgur, Phys. Rev. D **32**, 189 (1985); T. Barnes *et al.*, Phys. Rev. D **72**, 054026 (2005); T. Burch *et al.*, Phys. Rev. D **81**, 034508 (2010); L. Liu *et al.* (Hadron Spectrum Collaboration), JHEP **1207**, 126 (2012); N. Brambilla *et al.*, Eur. Phys. J. C **71**, 1534 (2011).

[5] C. H. Yu *et al.*, Proceedings of IPAC2016, Busan, Korea, 2016.
[6] X. Li *et al.*, Radiat. Detect. Technol. Methods **1**, 13 (2017); Y. X. Guo *et al.*, Radiat. Detect. Technol. Methods **1**, 15 (2017).
[7] M. Ablikim *et al.* (BESIII Collaboration), Nucl. Instrum. Meth. A **614**, 345 (2010).
[8] M. Ablikim *et al.* (BESIII Collaboration), Chin. Phys. C **41**, 013001 (2017).
[9] M. Ablikim *et al.* (BESIII Collaboration), Chin. Phys. C **42**, 023001 (2018).
[10] M. Ablikim *et al.* (BESIII Collaboration), Chin. Phys. C **37**, 123001 (2013).
[11] M. Ablikim *et al.* (BESIII Collaboration), Chin. Phys. C **41**, 063001 (2017).
[12] M. Ablikim *et al.* (BESIII Collaboration), Chin. Phys. C **39**, 093001 (2015).
[13] S. Kurokawa and E. Kikutani, Nucl. Instrum. Meth. A **499**, 1 (2003); T. Abe *et al.*, PTEP **2013**, 03A001 (2013).
[14] A. Abashian *et al.*, Nucl. Instrum. Meth. A **479**, 117 (2002); J. Brodzicka *et al.* (Belle Collaboration), PTEP **2012**, 04D001 (2012).
[15] E. Kou *et al.* (Belle II Collaboration), arXiv:1808.10567.
[16] V. V. Anashin *et al.*, Phys. Part. Nucl. **44**, 657 (2013).
[17] V. V. Anashin *et al.*, Phys. Lett. B **738**, 391 (2014).
[18] G. Apollinari *et al.*, CERN Yellow Report, 1 (2015).
[19] A. A. Alves *et al.* (LHCb Collaboration), JINST **3**, S08005 (2008); R. Aaij *et al.*, Int. J. Mod. Phys. A **30**, 1530022 (2015); Int. J. Mod. Phys. A **30**, 1530022 (2015).
[20] R. Aaij *et al.* (LHCb Collaboration), arXiv:1808.08865.
[21] V. V. Anashin *et al.* (KEDR Collaboration), Phys. Lett. B **711** 280 (2012).
[22] V. V. Anashin *et al.*, Phys. Lett. B **749**, 50 (2015).
[23] B. Aubert *et al.* (BABAR Collaboration), Phys. Rev. D **69**, 011103R (2004).
[24] G. S. Adams *et al.* (CLEO Collaboration), Phys. Rev. D **73**, 051103R (2006).
[25] M. Ablikim *et al.* (BESIII Collaboration), Phys. Lett. B **749**, 414 (2015).
[26] M. Ablikim *et al.* (BESIII Collaboration), Phys. Lett. B **761**, 98 (2016).
[27] M. Ablikim, *et al.* (BES Collaboration), Phys. Lett. B **659**, 74 (2008).
[28] L. Laudau, Phys. Abstr. A **52**, 125 (1949); C. N. Yang, Phys. Rev. **77**, 242 (1950).
[29] T. Appelquist and H. D. Politzer, Phys. Rev. Lett. **34**, 43 (1975); S. N. Gupta *et al.*, Phys. Rev. D **54**, 2075 (1996); D. Ebert *et al.*, Mod. Phys. Lett. A **18**, 601 (2003); W. L. Sang *et al.*, Phys. Rev. D **94**, 111501(R) (2016).
[30] M. Ablikim *et al.* (BESIII Collaboration), Phys. Rev. D **96**, 092007 (2017).
[31] R. Aaij *et al.* (LHCb Collaboration), Phys. Rev. Lett. **119**, 221801 (2017).
[32] D. Becirevic, F. Sanfilippo, J. High Energy Phys. **01**, 028 (2013).
[33] R. Aaij *et al.* (LHCb Collaboration), Phys. Lett. B **769**, 305 (2017).
[34] E. J. Eichten *et al.*, Phys. Rev. Lett. **89**,162002 (2002); P. Cho and M. B. Wise, Phys. Rev. D **51**, 3352 (1995).
[35] L. Antoniazzi *et al.* (E705 Collaboration), Phys. Rev. D **50**, 4258 (1994).
[36] E. Eichten *et al.*, Phys. Rev. D **17**, 3090 (1978); **21**, 203 (1980); S. Godfrey and N. Isgur, Phys. Rev. D **32**, 189 (1985); D. Ebert *et al.*, Phys. Rev. D **67**, 014027 (2003); M. Blank and A. Krassnigg, Phys. Rev. D **84**, 096014 (2011).
[37] M. Ablikim *et al.* (BESIII Collaboration), Phys. Rev. Lett. **115**, 011803 (2015).
[38] K. Chilikin *et al.* (Belle Collaboration), Phys. Rev. D **95**, 112003 (2017).
[39] K. A. Olive *et al.* (Particle Data Group), Chin. Phys. C **38**, 090001 (2014).
[40] K. Y. Liu, Z. G. He, and K. T. Chao, Phys. Rev. D **77**, 014002 (2008).